MALAYSIAN JOURNAL OF MICROSCOPY

Journal homepage: https://malaysianjournalofmicroscopy.org

RESEARCH ARTICLE

INVESTIGATION ON THE CRYSTALLOGRAPHY AND MORPHOLOGY OF LITHIUM COBALT MANGANESE TETROXIDE SYNTHESISED AT LOW TEMPERATURE WITH VARIOUS LITHIUM PRECURSORS

Tan Chee Wayne[1], Zul Hilmi Che Daud[2,*], Zainab Asus[2], Mohd Hasbullah Idris[1], Izhari Izmi Mazali[2], Mohd Kameil Abdul Hamid[1]

[1]Faculty of Mechanical Engineering, Universiti Teknologi Malaysia, 81310 Johor Bahru, Johor, Malaysia.

[2]Automotive Development Centre, Faculty of Mechanical Engineering, Universiti Teknologi Malaysia, 81310 Johor Bahru, Johor, Malaysia.

Abstract. Spinel structured lithium cobalt manganese tetroxide ($LiCoMnO_4$) which exhibit reduction potential ranging between 5.1 – 5.6 V (vs. Li^0 | Li^+) was identified to be one of the prospective cathode candidates for next generation lithium-ion electrochemical systems offering unprecedented voltage output. This article highlights the significance of lithium precursor towards the crystallography and morphology of lithium cobalt manganese tetroxide ($LiCoMnO_4$). $LiCoMnO_4$ cathode compounds in this research were synthesised via sol-gel reaction with stoichiometric ratio of Li:Co:Mn maintained at 1:1:1. The sol-gel formed were subsequently converted into xerogel before subjected to facile one-step low temperature calcination protocol at 600 ˚C. The source of lithium was derived from four distinctive precursors, namely lithium acetate dihydrate ($LiCH_3COO{\cdot}2H_2O$), lithium carbonate (Li_2CO_3), lithium fluoride (LiF) and lithium hydroxide monohydrate ($LiOH{\cdot}H_2O$) respectively. Co-existence of multiple phases were detected within the resultant compound synthesised with $LiCH_3COO{\cdot}2H_2O$, Li_2CO_3 and $LiOH{\cdot}H_2O$ being used as lithium precursor. X-ray diffraction coupled with Rietveld refinement revealed that single phase $LiCoMnO_4$ compound was attained from the post-calcinated specimen synthesised with LiF being used as the source of lithium. The adoption of LiF as lithium precursor also resulted in the formation of $LiCoMnO_4$ compound with relatively homogenized grain size as observed from field emission scanning electron microscopy (FESEM).

Keywords: $LiCoMnO_4$, cathode, sol-gel, calcination, crystallography.

Article Info

Received 17 February 2025
Accepted 15 September 2025
Published 4 December 2025

***Corresponding author: hilmi@mail.fkm.utm.my**

ISSN: 1823-7010, eISSN: 2600-7444

1. INTRODUCTION

Research efforts to enhance the operational voltage of rechargeable lithium-ion electrochemical systems through increased redox potential between electrodes has led to the emergence of three-dimensional (3D) spinel structured cathode active compounds as intercalation host with the presence of interstitial sites and pathways that facilitate ionic diffusion [1-3]. Whilst lithium manganese tetroxide ($LiMn_2O_4$) was identified to be the first spinel structured cathode compound developed to address the drawbacks possessed by the one-dimensional (1D) olivine and two-dimensional (2D) layered structured cathodes [4], various $Li\Omega_xMn_{2-x}O_4$ derivatives have been synthesised and investigated in the research laboratory settings.

The term "Ω" denotes low valance-state metal cations such as manganese (Mn) which may also be alternatively be substituted by cobalt (Co), nickel (Ni), chromium (Cr), aluminium (Al), magnesium (Mg), titanium (Ti), gallium (Ga), germanium (Ge), copper (Cu), zinc (Zn) and iron (Fe) [5,6]. Spinel structured lithium cobalt manganese tetroxide ($LiCoMnO_4$) which exhibit reduction potential ranging between 5.1 – 5.6 V (vs. Li^0 | Li^+) [7] was identified to be one of the prospective cathode candidates for next generation lithium-ion electrochemical systems offering unprecedented voltage output and energy density [5,8]. Moreover, it was also delineated via dilatometry that $LiCoMnO_4$ experience diminutive change in lattice parameter during intercalation and deintercalation of Li^+ ions, indicating the compound is dimensionally stable and could potentially be a viable cathode candidate for electrochemical systems with good cyclability [3, 9]. However, it was reported that $LiCoMnO_4$ often co-exist with secondary phase compounds especially when synthesized at high temperature due to lithium loss as well as deoxygenation mechanisms from the spinel lattice thereby induce reduction of Mn^{4+} ions to Mn^{3+} ions [10,11].

$LiCoMnO_4$ cathode compound have been fabricated at research laboratory since 1998 until the present time leveraging on various synthesis techniques ranging from solid-state reaction [12] to flux method [13], sol-gel [14], hydrothermal [15] as well as co-precipitation [16] with wide array of lithium precursors such as lithium carbonate (Li_2CO_3), lithium hydroxide monohydrate ($LiOH{\cdot}H_2O$), lithium chloride (LiCl), lithium nitrate ($LiNO_3$) and lithium acetate dihydrate ($LiCH_3COO{\cdot}2H_2O$) as well as lithium fluoride (LiF) which are more commonly used as additive as shown in Figure 1 [17]. Multiple research attempts to compensate oxygen loss experienced by $LiCoMnO_4$ synthesised in elevated temperature by performing calcination of the cathode active compound in oxygen enriched atmosphere as well as pure oxygen condition to produce Mn^{3+} free $LiCoMnO_4$ however unfortunately have not been proven to be effective [11].

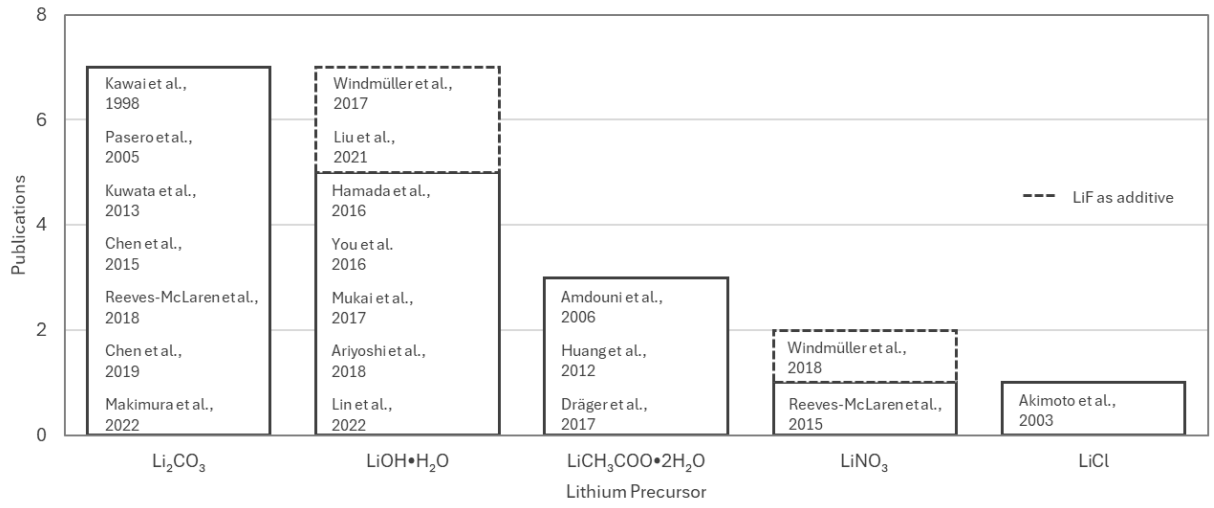

Figure 1: Lithium precursors used for the synthesis $LiCoMnO_4$

The decline in mass of $LiCoMnO_4$ induced by oxygen loss when subjected to high synthesis temperature as reported by Liu et al. in 2021 suggested that calcination of the cathode compound shall ideally not exceed the deterrent temperature limit of 600 ˚C [18] nor dwelled at prolonged duration [9] to prevent oxygen deficiency. It was also proposed that wet chemical synthesis techniques such as sol-gel and co-precipitation methods which require lower calcination temperature as well as fluorination [11] could potentially inhibit the formation of secondary phase compounds, yet in general still lack of research emphasis on the selection of lithium precursors used. Scarcity of lithium element and its derivatives in the universe as governed by Oddo-Harkins rule [19] as well as steep global demand for lithium-ion electrochemical systems to intensify the electrification of automotive sector calls for the necessity to diligently capitalise on the finite commodity. The focal point of this research is to investigate the significance of lithium precursor towards the resultant phase composition and corresponding crystallography of $LiCoMnO_4$. Sol-gel technique which offer homogenous mixing of reactants at molecular level, rapid crystal growth, narrow particle size distribution as well as high purity level and require relatively lower calcination temperature will be adopted as the synthesis methodology in this research [20,21].

2. METHODS AND MATERIALS

2.1 Synthesis

Lithium precursors used in this study were derived from four distinctive compounds, namely lithium acetate dihydrate ($LiCH_3COO{\cdot}2H_2O$), lithium carbonate (Li_2CO_3), lithium fluoride (LiF) and lithium hydroxide monohydrate ($LiOH{\cdot}H_2O$). The source of cobalt and manganese on the other hand were derived from cobalt (II) acetate tetrahydrate ($Co(CH_3COO)_2{\cdot}4H_2O$) and manganese (II) acetate tetrahydrate ($Mn(CH_3COO)_2{\cdot}4H_2O$) respectively. The reactants were formulated to attain stoichiometric ratio of Li:Co:Mn = 1:1:1 and completely hydrolyzed in de-ionized water. Citric acid monohydrate ($C_6H_8O_7{\cdot}H_2O$) which served as chelating agent was added into the homogenised mixture at molar ratio of $N_{(C_6H_8O_7{\cdot}H_2O)}/N_{cations}$ = 2 without controlling the pH value of the solution. The solution was subsequently heated to 90°C and mechanically stirred at 500 rpm for approximately 1.5 hours until integrated gelation network formed. Sol-gel formed was subsequently subjected to dehydration process in a forced convection oven operated at 90 °C for 12 hours to remove residual moisture. Dehydrated xerogel was transferred into 150 ml capacity alumina crucible followed by calcination in a muffle furnace with effective chamber volume of 200 mm × 300 mm × 120 mm. Calcination was performed at heating rate of 10 °C/min to target temperature of 600 °C and dwelled for 12 hours followed by natural cooling to room temperature without facilitated by additional oxygen supply nor air circulation. The post-calcinated compounds were subjected to 10 hours of continuous pulverisation by overfall ball milling in a ∅100 mm × 100 mm cylindrical vessel with ∅10 mm zirconia milling media. Rotational speed of the milling vessel was fixed at 60 rpm, while mass ratio of milling media:cathode active material was set at 10:1. Figure 2 illustrates the sequence for the synthesis of $LiCoMnO_4$ cathode compound.

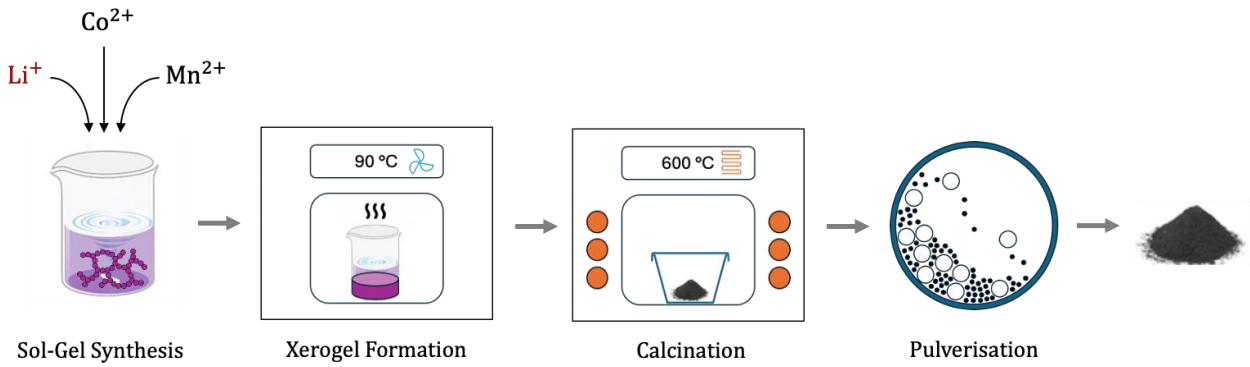

Figure 2: Illustration of synthesis sequence

2.2 Characterisation

Crystallographic analysis was performed on the pulverised compounds via powder x-ray diffraction (XRD, Rigaku Smartlab) technique with Cu-K_α radiation operated at 40 kV and 40 mA. X-ray diffraction patterns of the resultant compounds were collected at 2θ angle ranging between 10 ° – 100 ° at 0.01 ° step width and scanning rate of 1 °/min. Mass fraction of resultant phases present within the post-calcinated were quantified via Rietveld refinement method with PDXL software package coupled with ICDD PDF4 database. Microstructure of the synthesised compounds were inspected via Field Emission Scanning Electron Microscopy (FESEM, Hitachi SU8020) and Energy Dispersive X-ray Spectroscopy (EDS, Oxford Instruments X-Max) at ×30000 magnification in Secondary Electron mode at 30 Pa, 5 kV and 40 % probe current.

3. RESULTS AND DISCUSSION

3.1 Crystallography

X-ray diffraction patterns of the resultant compounds synthesised via sol-gel technique with 4 distinctive lithium precursors and subsequently subjected to identical calcination protocol were depicted in Figure 3.

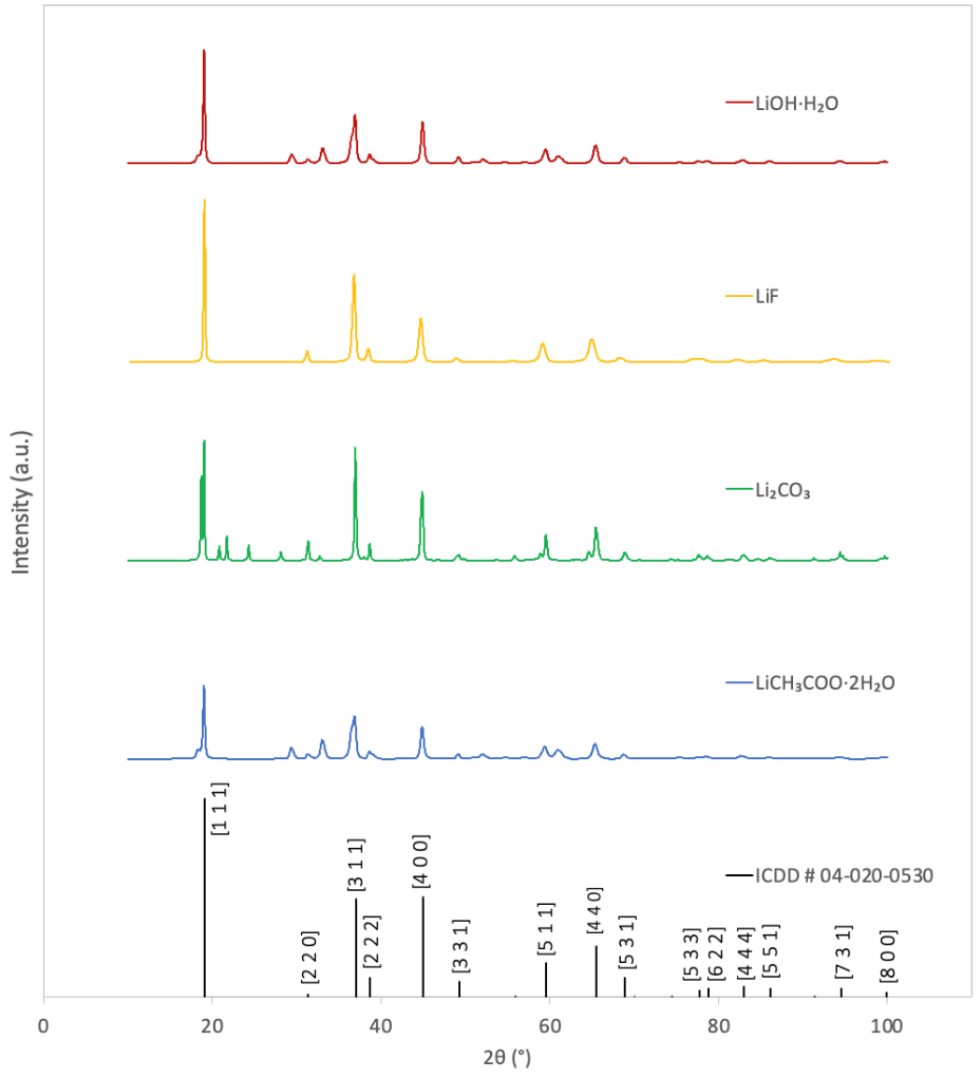

Figure 3: X-ray diffraction pattern

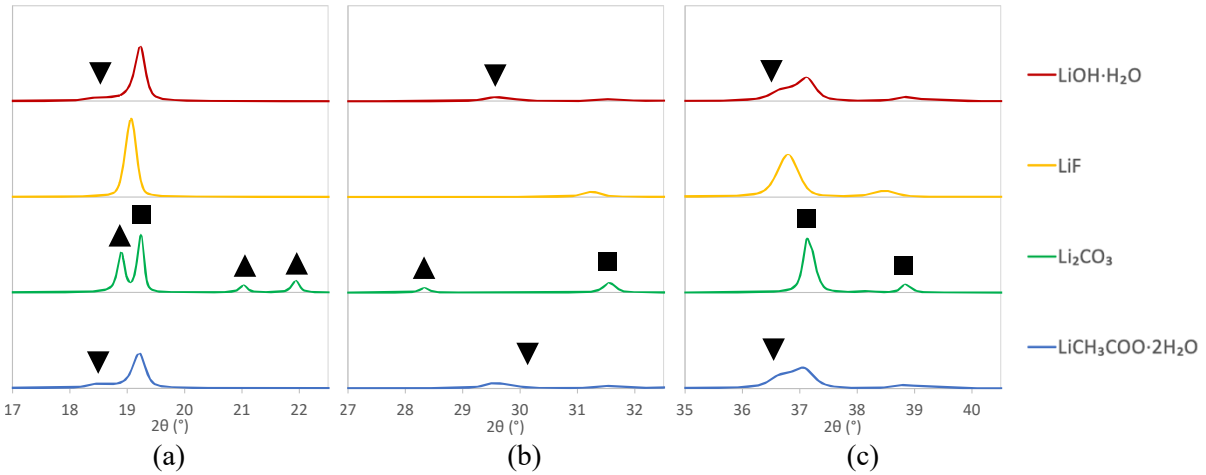

Figure 4: Diffractogram focused at (a) 17°-22°, (b) 27°-32° and (c) 35°-40°

At a glance, it was apparent that all of the post-calcinated compounds displayed x-ray diffractogram with well-defined peaks, suggesting the formation of well-crystallised resultant compounds. Nonetheless, meticulous observation on the close-up diffractogram as shown in Figure 4 as well as phase quantification via Rietveld refinement analysis with uncertainty reported in bracket as shown in Figure 5 divulged that only the category of specimen that was synthesised with LiF as precursor attained single phase resultant compound. The diffractogram can be closely indexed to the cubic space group $Fd\bar{3}m$ spinel crystal structure resembling ICDD # 04-020-0530 and diffraction pattern of single crystal $LiCoMnO_4$ synthesised by Hamada et al. via flux method [13].

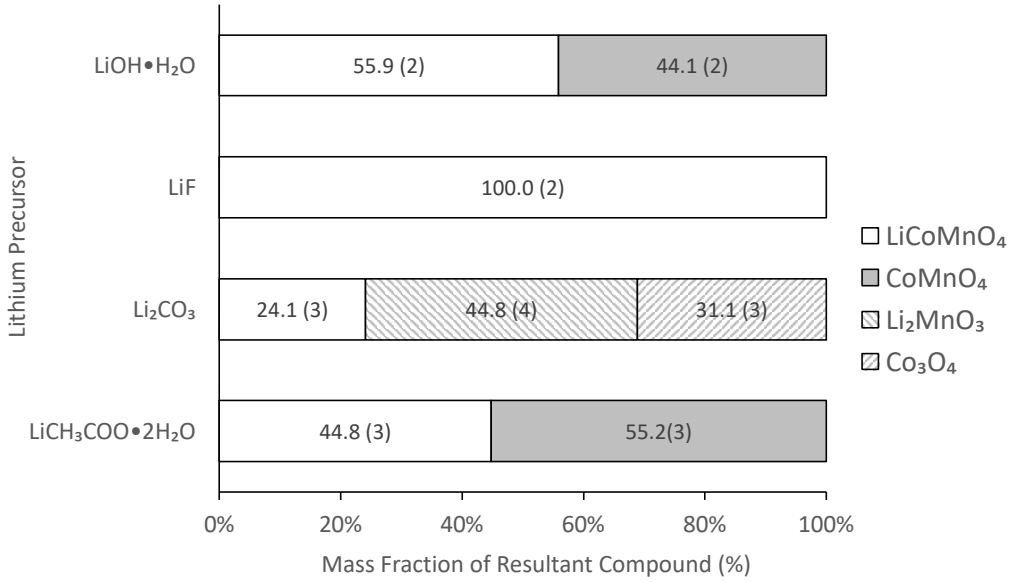

Figure 5: Resultant phase composition

Intense x-ray diffraction peaks were observed at 2θ angle of 19.1°, 36.8° and 44.7° proximity corresponding to the [1 1 1], [3 1 1] and [4 0 0] crystal plane in the cubic spinel structure of the resultant compound synthesised with LiF as lithium precursor. Meanwhile, prominent x-ray diffraction peaks were also detected at 2θ angle of 38.5°, 48.9°, 59.1°, 64.9° as well as 68.3° corresponding to [2 2 2], [3 3 1], [5 1 1], [4 4 0] and [5 3 1] crystal plane in the cubic spinel structure.

It may be distinguished from the close-up diffractogram as shown in Figure 4 that the resultant compounds synthesised with $LiCH_3COO{\cdot}2H_2O$ and $LiOH{\cdot}H_2O$ both exhibit minor peaks at 2θ angle of 18.5°, 29.5° and 37.2° proximity. The detection of minor peaks was attributed by the co-existence of lithium deficient $CoMnO_4$ (▼) which may be potentially ascribable to the hygroscopic nature of both hydrated lithium compounds used as the precursors in this investigative experiment.

It was speculated that both hydrated lithium compounds readily absorb moisture from surrounding and caused deprivation of Li^+ atoms within the sol-gel system despite gravimetric proportion of reactants were precisely controlled to achieve stoichiometric of Li:Co:Mn = 1:1:1 for each of the experiments. Nonetheless, high hydrosolubility properties of both $LiCH_3COO{\cdot}2H_2O$ and $LiOH{\cdot}H_2O$ lithium precursors still possessed well-grounded practical benefits shall $LiCoMnO_4$ cathode active material were to be scaled up for high volume manufacturing via similar synthesis technique due to the potential opportunities for lower water and energy consumption as well as improved cost effectiveness. Materials storage and handling condition of lithium precursor with hygroscopic properties may be further improved in the future to control moisture uptake, while the dosage of lithium precursors may be adequately optimized as necessary to compensate for water absorption from surroundings.

Meanwhile, it was observed that the formation of $LiCoMnO_4$ only made up of less than a quarter of the total composition from the resultant compounds synthesised with Li_2CO_3 as lithium precursor and were accompanied by the presence of multiple undesirable chemical by-products particularly rock-salt phase Li_2MnO_3 (▲) which are commonly reported by various researchers working on similar topics [10, 22-25] as well as Co_3O_4 (■) [15, 26, 27]. Unlike other lithium precursors with hygroscopic issue as discussed earlier, the solubility limit of Li_2CO_3 in water drastically reduced with increased temperature [28]. Partial re-precipitation of the carbonate-based precursor may potentially occur as temperature of the homogenised colloidal solution was elevated to 90 °C during sol-gel reaction. The presence of unreacted Li_2CO_3 within xerogel formed upon dehydration process may subsequently undergo thermal decomposition and react unfavorably during calcination.

The resultant compound synthesised with LiF used as lithium precursor exhibit cubic space group $Fd\bar{3}m$ spinel crystal structure with lattice parameter of a = b = c = 8.053 Å which is comparable to the reported values from the $LiCoMnO_4$ specimens prepared by various researchers [8, 13, 18]. The weighted residual error (R_{wp}), residual error (R_p) and fit indicator (S) index reported to be 2.60 %, 1.79 % and 1.87 respectively. Other important information on the crystal structure of $LiCoMnO_4$ compound synthesised with LiF as the source of lithium were refined with $(Li_{1-x}Co_x)_{8a}[Co_{1-x}MnLi_x]_{16d}O_4$ structural model [8, 13] and outlined in Table 1.

Table 1: Structural parameters of $LiCoMnO_4$ synthesised with LiF as lithium precursor

Atom	Wyckoff Position	x	y	z	Occupancy
Li	8a	0.125	0.125	0.125	0.620
Co1	8a	0.125	0.125	0.125	0.380
Co2	16d	0.500	0.500	0.500	0.345
Mn	16d	0.500	0.500	0.500	0.655
O	32e	0.254	0.254	0.254	1.000

It was reported that lithium ions present within the synthesised $LiCoMnO_4$ only located at the tetrahedral 8a sites which concurred with the findings observed by Mukai et al. in 2017 [23]. However, the occupancy index of lithium ions in 8a sites is relatively low as compared to the values reported by other researchers [8,13,18,21,23] on pristine state $LiCoMnO_4$ before subjected to charging due to higher

distribution of cobalt ions at 8a sites. Cobalt ions which may display multiple of oxidation states are also partially distributed in octahedral 16d sites along with manganese ions potentially due to the occurrence of cationic mixing [29]. Meanwhile, oxygen anions are located at the 32e sites with oxygen positional parameter, u of 0.254.

The crystallite size, D of $LiCoMnO_4$ synthesised with LiF as lithium precursor was estimated to be 35.9 nm using Scherrer's formula as shown in equation 1 [29]. Dimensionless shape factor, k of 0.94 and x-ray wavelength, λ of 1.5406 Å [30] were applied to the equation corresponding to the Cu-K_α radiation used. Meanwhile, the full width at half maximum (FWHM), B in radian as well as Bragg angle, θ at the maximum peak intensity were deconvoluted with OriginPro software package to compute the crystallite size.

$$D = \frac{K\lambda}{B\cos\theta} \quad (1)$$

3.2 Morphology

Morphology evaluation performed via field emission scanning electron microscopy (FESEM) as shown in Figure 6(a) inferred that the adoption of LiF as lithium precursor resulted in the formation of single-phase compound with relatively homogenized grain size.

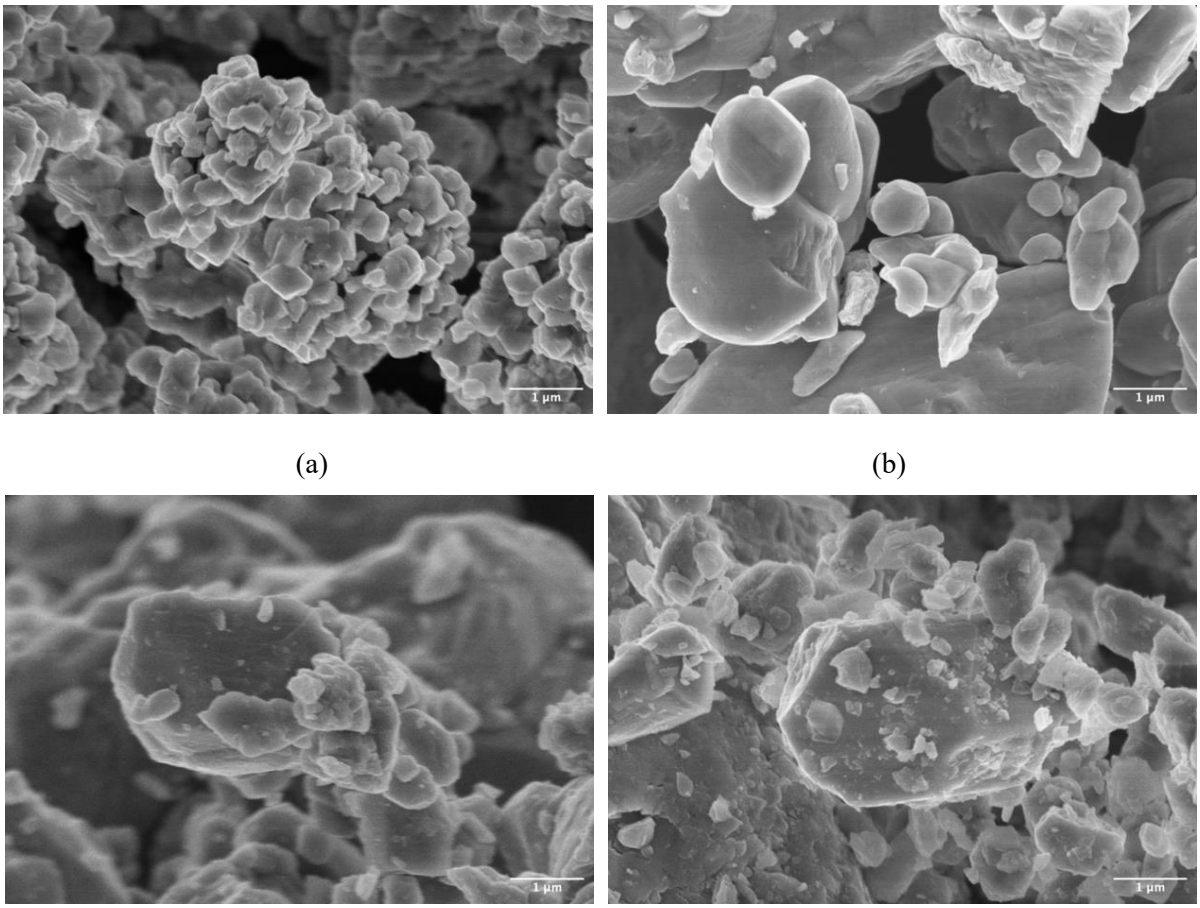

(a) (b)

(c) (d)

Figure 6: Microstructure of $LiCoMnO_4$ synthesised with (a) LiF, (b) $LiCH_3COO{\cdot}2H_2O$, (c) $LiOH{\cdot}H_2O$ and (d) Li_2CO_3 as lithium precursor

Nonetheless, aggregation of $LiCoMnO_4$ particles was also discerned from microstructural image, suggesting further optimisation of parameters on calcination or pulverisation process may be required. Meanwhile, co-existence of multiple phases with irregular particle shapes and sizes were observed from the morphology of resultant compounds synthesized with $LiCH_3COO{\cdot}2H_2O$, $LiOH{\cdot}H_2O$ and Li_2CO_3 being used as the source of lithium. The observation of impurity phases as shown in Figure 6(b), 6(c) & 6(d) also aligned with the findings from x-ray diffraction analysis which was discussed earlier in section 3.1.

Energy Dispersive X-ray Spectroscopy (EDS) analysis was also performed on the resultant compound synthesised with the source of lithium derived from LiF. The EDS spectrum as shown in Figure 7 validated that the atomic ratio of Co:Mn of the resultant compound is close to 1:1 as intended by formulation [30].

The element of lithium was not discernible from the spectrum due to extremely weak x-ray beam produced by the element as well as limitation of ordinary EDS system with detector window which exhibit the tendency to absorb the signal as expected based on empirical finding presented earlier by other researchers working on other spinel structured cathode compounds such as $LiNi_{0.5}Mn_{1.5}O_4$ [30]. Meanwhile, elemental mapping outcome as depicted in Figure 8 also inferred homogenous distribution of Co, Mn, O and F throughout the resultant compound.

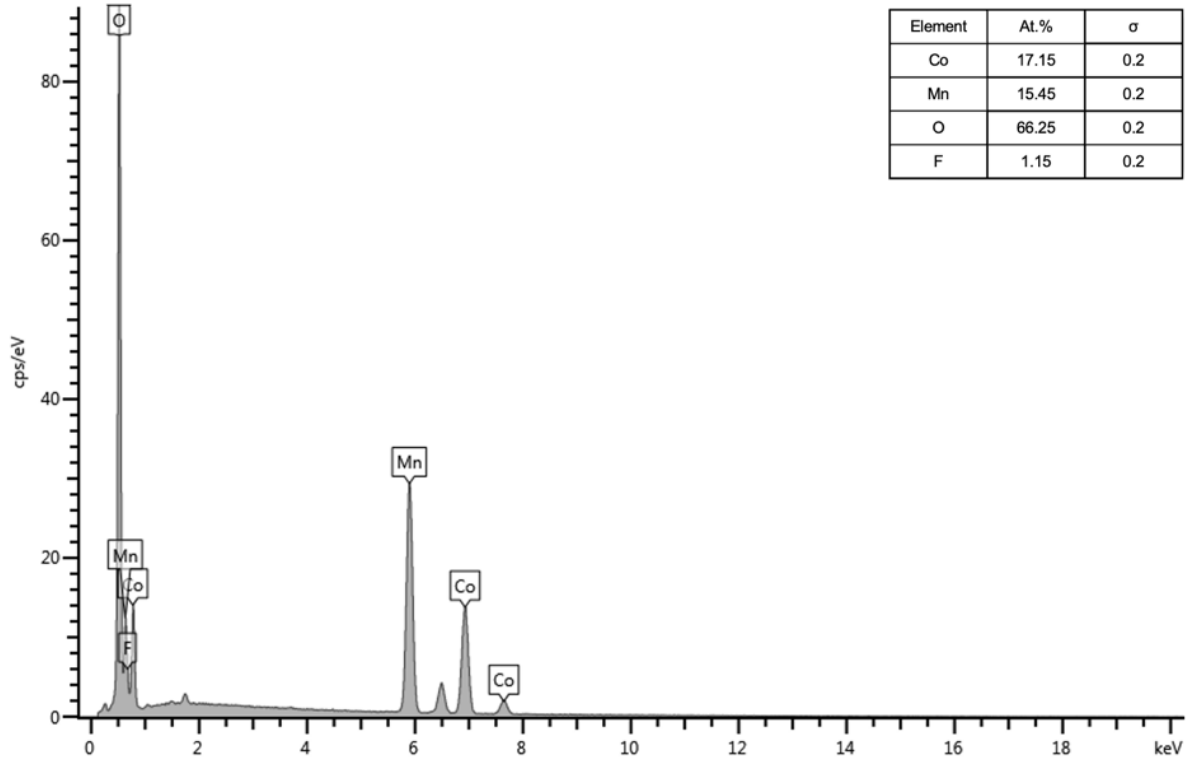

Element	At.%	σ
Co	17.15	0.2
Mn	15.45	0.2
O	66.25	0.2
F	1.15	0.2

Figure 7: EDS spectrum of $LiCoMnO_4$ synthesised with LiF as lithium precursor

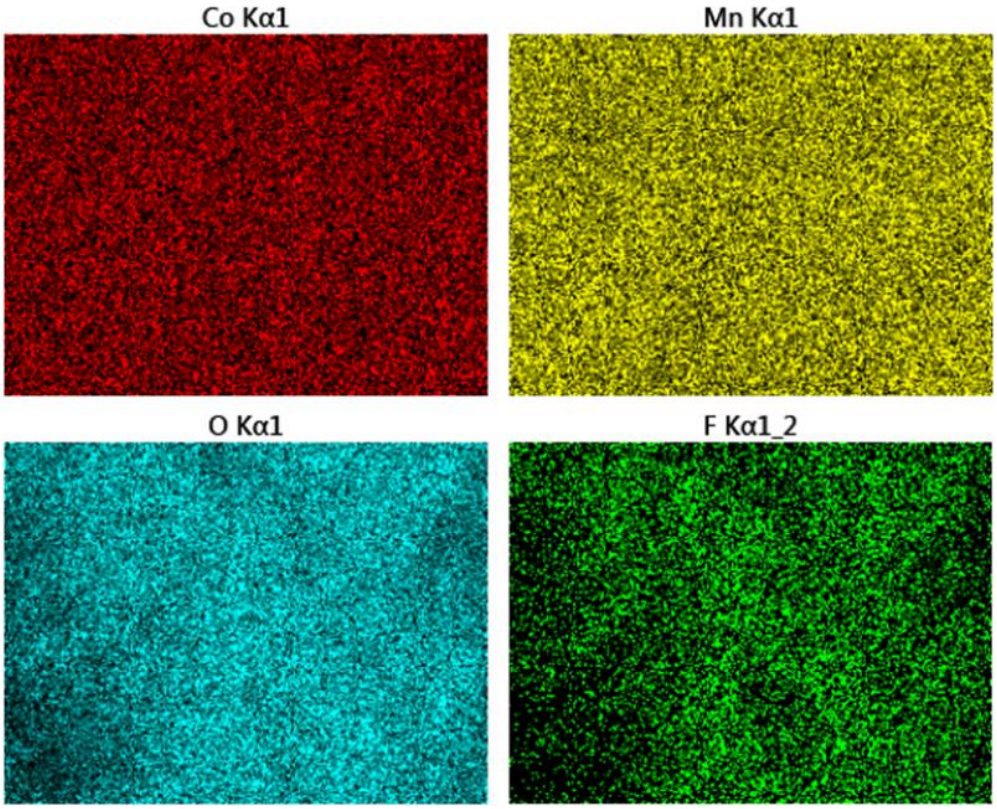

Figure 8: Elemental mapping of $LiCoMnO_4$ synthesised with LiF as lithium precursor

4. CONCLUSIONS

In summary, it may be concluded that the selection of lithium precursor possessed significant influence on the crystallography and morphology of $LiCoMnO_4$. It was empirically demonstrated that the employment of non-hydrated LiF as lithium precursor has enabled the formation of single-phase spinel structured $LiCoMnO_4$ cathode active compound after subjected to calcination at 600 °C as inferred by phase quantification via X-ray Diffraction (XRD) coupled with Rietveld refinement analysis with well-homogenised grain size as observed from microstructural image captured by Field Scanning Electron Microscopy (FESEM).

The technical viability of further reducing the calcination temperature with the source of lithium derived from LiF will be evaluated and the calcination temperature range which enabled the formation of single-phase $LiCoMnO_4$ will be defined soon. Correlation between calcination temperature and the crystallography and granulometry of the resultant $LiCoMnO_4$ compound synthesised with LiF as lithium precursor as well as the corresponding impacts on electrochemical performance shall also be established.

Acknowledgements

The research was funded by a grant from UTM Research University Grant (UTM Matching Grant: Q.J130000.3024.04M84).

Author Contributions

All authors contributed toward data analysis, drafting and critically revising the paper and agree to be accountable for aspects of the work.

Disclosure of Conflict of Interest

The authors have no disclosures to declare.

Compliance with Ethical Standards

This work is compliant with ethical standards.

References

[1] Julien, C., Mauger, A., Vijh, A. & Zaghib, K. (2015). *Lithium Batteries: Science and Technology*. (Springer International Publishing) pp. 69-72.

[2] Marom, R., Amalraj, S. F., Leifer, N., Jacob, D. & Aurbach, D. (2011). A review of advanced and practical lithium battery materials. *Journal of Materials Chemistry. 21(27)*, 9938-9954.

[3] Reeves-McLaren, N., Hong, M., Alqurashi, H., Xue, L., Sharp, J., Rennie, A. J. & Boston, R. (2018). The spinel $LiCoMnO_4$: 5 V cathode and conversion anode. In Proceedings of the 3rd Annual Conference in Energy Storage and Its Applications (3rd CDT-ESA-AC), Sheffield, 11-12 Sept 2018.

[4] Kebede, M. A. & Ezema, F. I. (2019). *Electrochemical Devices for Energy Storage Applications*. (CRC Press) pp. 2-17.

[5] Julien, C. M. & Mauger, A. (2013). Review of 5-V electrodes for li-ion batteries: status and trends. *Ionics. 19(7)*, 951-988.

[6] Akimoto, J., Gotoh, Y. & Takahashi, Y. (2003). Crystal growth of spinel-type $LiM_xMn_{2-x}O_4$ (M = Cr, Co, Ni) in high-temperature molten chlorides. *Crystal Growth & Design. 3(5)*, 627-629.

[7] Makimura, Y., Niitani, K., Goto, I., Tsujiko, A., Oka, H., Nonaka, T. & Abe, T. (2022). Improved kinetics in spinel-related 5 V positive electrode materials by changing lithium insertion schemes for lithium-ion batteries. *ACS Applied Energy Materials. 5(10)*, 12239-12251.

[8] Dräger, C., Sigel, F., Indris, S., Mikhailova, D., Pfaffmann, L., Knapp, M. & Ehrenberg, H. (2017). Delithiation/relithiation process of $LiCoMnO_4$ spinel as 5 V Electrode Material. *Journal of Power Sources. 371*, 55-64.

[9] Ariyoshi, K., Yamamoto, H. & Yamada, Y. (2018). High dimensional stability of $LiCoMnO_4$ as positive electrodes operating at high voltage for lithium-ion batteries with a long cycle life. *Electrochimica Acta. 260*, 498-503.

[10] Ariyoshi, K., Yamamoto, H. & Yamada, Y. (2021). Synthesis optimization of electrochemically active $LiCoMnO_4$ for high-voltage lithium-ion batteries. *Energy & Fuels. 35(16)*, 13449-13456.

[11] Windmüller, A., Tsai, C.L., Möller, S., Balski, M., Sohn, Y. J., Uhlenbruck, S. & Guillon, O. (2017). Enhancing the performance of high-voltage $LiCoMnO_4$ spinel electrodes by fluorination. *Journal of Power Sources. 341*, 122-129.

[12] Kawai, H. (1999). A new lithium cathode $LiCoMnO_4$: Toward practical 5 V lithium batteries. *Electrochemical and Solid-State Letters. 1(5)*, 212-214.

[13] Hamada, Y., Hamao, N., Kataoka, K., Ishida, N., Idemoto, Y. & Akimoto, J. (2016). Single crystal synthesis, crystal structure and electrochemical property of spinel-type $LiCoMnO_4$ as 5 V positive electrode materials. *Journal of the Ceramic Society of Japan. 124(6)*, 706-709.

[14] Huang, X., Lin, M., Tong, Q., Li, X., Ruan, Y. & Yang, Y. (2011). Synthesis of LiCoMnO4 via a sol–gel method and its application in high power $LiCoMnO_4/Li_4Ti_5O_{12}$ lithium-ion batteries. *Journal of Power Sources. 202*, 352-356.

[15] You, M., Huang, X., Lin, M., Tong, Q., Li, X., Ruan, Y. & Yang, Y. (2016). Preparation of $LiCoMnO_4$ assisted by hydrothermal approach and its electrochemical performance. *American Journal of Engineering and Applied Sciences. 9(2)*, 396-405.

[16] Lin, H.F., Tsai, Y.R., Cheng, C.H., Cheng, S.T., Chen, D.Z. & Wu, N.Y. (2022). Structural and electrochemical properties of $LiCoMnO_4$ doped with Mg, La, and F as a high-voltage cathode material for lithium ion batteries. *Electrochimica Acta. 427*, 140904.

[17] Tan, C. W., Che Daud, Z. H., Asus, Z., Idris, M. H., Mazali, I. I., Ardani, M. I. & Abdul Hamid, M. K. (2022). A holistic review on the synthesis techniques of spinel structured lithium cobalt manganese tetroxide. *Journal of Metals, Materials and Minerals. 32(4)*, 59-70.

[18] Liu, S., He, H. & Chang, C. (2021). Understanding the improvement of fluorination in 5.3 V $LiCoMnO_4$ spinel. *Journal of Alloys and Compounds. 860*, 158468.

[19] Mae, Y. (2017). Neutron multiple number as a factor ruling both the abundance and some material properties of elements. *Journal of Materials Science Research. 6(3)*, 37-42.

[20] Danks, A. E., Hall, S. R. & Schnepp, Z. (2016). The evolution of 'sol–gel' chemistry as a technique for materials synthesis. *Materials Horizons. 3(2)*, 91-112.

[21] Amdouni, N., Gendron, F., Mauger, A., Zarrouk, H. & Julien, C. M. (2022). $LiMn_{2-y}Co_yO_4$ ($0 \leq y \leq 1$) Intercalation compounds synthesized from wet chemical route. *Materials Science and Engineering: B. 129(1-3)*, 64-75.

[22] Zhou, J.E., Chen, J., Zhang, X., Zeb, A. & Lin, X. (2022). Molecular and atomic manipulation of metal-organic framework-derived $LiCoMnO_4$: An oxygen-deficient strategy for advanced lithium storage. *Journal of Energy Chemistry. 75*, 216-228.

[23] Mukai, K. & Uyama, T. (2017). Toward positive electrode materials with high-energy density: electrochemical and structural studies on $LiCo_{(x)}Mn_{(2-x)}O_{(4)}$ with $0 \leq x \leq 1$. *ACS Omega. 2(8)*, 5142-5149.

[24] Pasero, D., de Souza, S., Reeves, N. & West, A. R. (2005). Oxygen content and electrochemical activity of $LiCoMnO_{4-\delta}$. *Journal of Materials Chemistry. 15(41)*, 4435-4440.

[25] Chen, L., Fan, X., Hu, E., Ji, X., Chen, J., Hou, S., Deng, T., Li, J., Su, D., Yang, X. & Wang, C. (2019). Achieving high energy density through increasing the output voltage: A highly reversible 5.3 V battery. *Chem. 5(4)*, 896-912.

[26] Reeves-McLaren, N., Sharp, J., Beltran-Mir, H., Rainforth, W. M. & West, A. R. (2015). Spinel-rock salt transformation in $LiCoMnO_{4-\delta}$. *Proceedings of the Royal Society A. 472(2185)*, 20140991.

[27] Windmüller, A., Bridges, C. A., Tsai, C.-L., Lobe, S., Dellen, C., Veith, G. M., Finsterbusch, M., Uhlenbruck, S. & Guillon, O. (2018). Impact of fluorination on phase stability, crystal chemistry, and capacity of $LiCoMnO_4$ high voltage spinels. *ACS Applied Energy Materials*. *1(2)*, 715-724.

[28] Han, B., Anwar Ui Haq, R. & Louhi-Kultanen, M. (2020). Lithium carbonate precipitation by homogeneous and heterogeneous reactive crystallization. *Hydrometallurgy. 195*, 105386.

[29] Rahim, A. S., Aziz, N., Nor, N. A. M. & Osman, Z. (2020). $LiNi_{0.5}Mn_{1.5}O_4$ cathode material prepared by sol–gel method. *Molecular Crystals and Liquid Crystals. 695(1)*, 10-18.

[30] Radzi, Z. I., Balakrishnan, V., Pandey, A. K., Kufian, M. Z., Rahim, N. A., Raihan, S. R. S. & Ramesh, S. (2022). Structural, electrical and electrochemical characterization of hybrid morphological $LiN_{i0.5}Mn_{1.5}O_4$ cathode material. *Physica B: Condensed Matter. 624(10)*, 413376.